Lidar measurements of ozone vertical profiles

Gerard J. Megie, Gerard Ancellet, and Jacques Pelon

Remote measurements of trace constituents using an active technique such as lidar have been made possible for the rapid development of powerful tunable laser sources. This paper, originally presented at the OSA Topical Meeting on Optical Remote Sensing of the Atmosphere, in January 1985, illustrates the differential absorption lidar technique used for the measurement of the ozone vertical distribution in the troposphere and the atmosphere.

I. Introduction

The behavior of trace constituents in the earth's upper atmosphere, governed by chemical, dynamical, and radiative processes, is of particular importance for the overall balance of the stratosphere and mesosphere. In particular ozone plays a dominant role by absorbing the short-wavelength UV radiation which might damage living organisms and by maintaining the radiative budget equilibrium.

Continuous monitoring of ozone and other minor constituents in the earth's stratosphere and troposphere is of particular interest in present-day atmospheric physics, as the potential modification of the ozone layer due to man's activities can greatly modify the earth's environment and climate; the measurement of the total ozone column content and vertical profile by a ground-based UV spectrometer network or by satellite-borne systems remains the fundamental basis for global observations and trend analysis. However the required accuracy of these measurements will also imply in the future the operation of new active systems, such as lidar, which could provide a high degree of reliability in terms of accuracy and absolute precision. Furthermore the very large variability of the ozone number density in the troposphere and lower stratosphere and at the boundary between these two regions and its interpretation in terms of horizontal and vertical transport requires high spatial and temporal resolution measurements which are presently beyond the possibilities of passive systems.

Remote measurements of trace constituents using an active technique such as lidar have been made possible by the rapid development of powerful tunable laser sources which have opened a new field in atmospheric spectroscopy by providing sources which can be tuned to characteristic spectral features of atmospheric constituents. The interaction of a laser beam with the atmosphere is in principle dominated at all wavelengths by elastic processes, i.e., Rayleigh scattering from atmospheric gas molecules and Mie scattering due to particles of different natures and shapes. However, considering the simplified lidar equation

$$n_r = n_0 \cdot \frac{A_0}{R^2} (\beta_R + \beta_M + \beta_i) \cdot \Delta R \cdot \exp[-2(\tau_R + \tau_M + \tau_i)], \quad (1)$$

(where n_0 and n_r are the number of photons emitted and received per pulse from range R; A_0 is the receiver area; β_R, β_M, and β_i are the volume backscattering coefficients for Rayleigh scattering, Mie scattering, and resonant scattering by a given species i; τ_R, τ_M, and τ_i being the corresponding optical thickness for the path length R; ΔR is the range resolution), the determination of a given constituent number density N_i is then possible by two means: either β_i is much larger than $\beta_R + \beta_M$ allowing the measurement of N_i based on a scattering process, or τ_i is much larger or of the same order of magnitude as $\tau_r + \tau_m$ allowing the measurement of N_i based on an absorption process.

This paper illustrates the second method known as the differential absorption lidar technique (DIAL) as it has been used for the measurement of the ozone vertical distribution in both the troposphere and stratosphere.

The recent development of the DIAL technique[1] for stratospheric applications has allowed during the last seven years a very rapid growth in lidar observations of the ozone vertical distribution from the ground up to the 50-km altitude level. The purpose of this review paper is to give a rapid analysis of the method itself and to describe the various systems which have been in operation at the Observatoire de Haute Provence since 1980. An analysis of their advantages and disadvantages with respect to one another will also be presented and an overview of already obtained data will be given.

The authors are with Service d'Aeronomie du CNRS, 91371 Verrieres le Buisson, France.

Received 23 May 1985.
0003-6935/85/213454-10$02.00/0.

Perspectives in terms of ozone monitoring will be considered in the last subsection.

II. Methodology—the DIAL Technique

The basic principles of the differential absorption laser technique have been described by various authors.[1,2] Its application to ozone measurements for both UV and IR systems has been analyzed by Megie and Menzies.[3] They concluded that as far as higher tropospheric and stratospheric measurements are concerned the UV wavelength range is the best candidate for ground-based observations. Therefore only such systems operating in the Hartley-Huggins bands of ozone between 280 and 320 nm will be considered here. The forthcoming analysis will follow the study made by Pelon and Mégie.[4]

The usual lidar equation which relies on the total number $n_{\lambda R}$ of backscattered photoelectrons at wavelength λ from the cell at range R and of thickness ΔR to the number of emitted photons in the laser pulse at wavelength λ is written as

$$n_{\lambda R} = n_{e\lambda} \cdot \Delta R \cdot \frac{A_0}{R^2} \beta_{\lambda R} \cdot \xi \cdot \xi' \cdot \exp[-2(\tau^o_{\lambda R} + \tau^e_{\lambda R})], \quad (2)$$

where $\beta_{\lambda R}$ is the atmospheric backscattering coefficient at wavelength λ and range R;

ΔR is the thickness of the range cell corresponding to a time gate interval of $2\Delta R/c$ generally larger than the pulse duration τ_L;

A_0 is the receiver area;

ξ is the detector efficiency;

ξ' is the optical efficiency of the transmitter–receiver system;

$\tau^o_{\lambda R}$ is the integrated optical thickness due to absorption by the constituent under study, i.e., ozone:

$$\tau^o_{\lambda R} = \int_0^R \sigma_{\lambda R} N_0(R) dR, \quad (3)$$

where $\sigma_{\lambda R}$ is the ozone absorption cross section and $N_0(R)$ is the ozone number density;

$\tau_{\lambda R}{}^e$ is the integrated optical thickness excluding absorption by ozone; and

$\tau_{\lambda R}$ is the total integrated optical thickness $\tau_{\lambda R} = \tau_{\lambda R}{}^o + \tau_{\lambda R}{}^e$.

If one considers the ratio of the two backscattered signals corresponding to two successive cells R_1 and $R_2 = R_1 + \Delta R$ for the same laser pulse, one can write

$$\Delta\tau^o_{\lambda 1} = \frac{1}{2} \ln \frac{n_{\lambda 1}}{n_{\lambda 2}} + \ln \frac{\beta_{\lambda 2} R_1^2}{\beta_{\lambda 1} R_1^2} - \Delta\tau^e_{\lambda 1}, \quad (4)$$

where $\Delta\tau_{\lambda R}$ is defined as the local optical thickness of the constituent within the range cell R, $R + \Delta R$. Assuming the knowledge of the ozone absorption cross section $\sigma_{\lambda R}$ at this range, $\Delta\tau^o_{\lambda R}$ is then directly proportional to the average ozone number density within the same range cell as

$$\Delta\tau^o_{\lambda R} = \sigma_{\lambda R} \cdot N_0(R) \cdot \Delta R. \quad (5)$$

Thus a one-wavelength lidar measurement can lead to the determination of the ozone vertical profile from the laser backscattered signals $n_{\lambda 1}, n_{\lambda 2}$ if the last two terms of Eq. (4) are known. If one assumes a pure molecular scattering atmosphere (no aerosol particles), $\beta_{\lambda R}$ and $\Delta\tau_{\lambda R}{}^e$ are then proportional to the atmosphere number density as the Rayleigh scattering process is the only one contributing to the laser light scattering. Thus using an atmospheric model or the atmospheric parameters as given by local radiosonde measurements such a technique can be used for ozone profiling.[5] However aerosol particles are always present in the troposphere and in the lower stratosphere around 20 km and their abundance can be greatly increased by more than 1 order of magnitude during the one to two years following large volcanic eruptions.[6] Then single wavelength measurements cannot be considered as fully reliable for any atmospheric situation and one has to use a second wavelength λ_2 different from λ_1 to discriminate the ozone absorption from other potential interfering species. Writing Eq. (4) for a second wavelength λ_2 and taking the difference lead to

$$\Delta\tau_{1R} - \Delta\tau_{2R} = \ln \frac{n_{22} n_{11}}{n_{12} n_{21}} + \ln \frac{\beta_{12} \beta_{21}}{\beta_{L11} \beta_{22}}, \quad (6)$$

where the first subscript refers to the wavelength and the second, when present, to the range.

The signal-to-noise ratio $S_{\lambda R}$ for a single wavelength measurement is given for an incoherent detection scheme and assuming that the fluctuations of the various sources of the photodetector current are governed by Poisson statistics by

$$S_{\lambda R} = \frac{n_{\lambda R}}{(n_{\lambda R} + n_B + n_D)^{1/2}}, \quad (7)$$

where n_B is the number of background photons and n_D is the square of the photodetector dark current fluctuations within the time gate interval $2\Delta R/c$.

In the usual derivation of the DIAL method, one considers that the wavelength variations of $\beta_{\lambda R}$ and $\tau_{\lambda R}{}^e$ between λ_1 and λ_2 contribute only to the systematic error term ϵ_2 (see below)[7] so that Eq. (6) can be rewritten as

$$\Delta\tau^o_{1R} - \Delta\tau^o_{2R} = \frac{1}{2} \ln \frac{n_{22} n_{11}}{n_{12} n_{21}}. \quad (8)$$

The average ozone number density $N_0(R)$ within the range cell R, $R + \Delta R$ is then given by

$$N_0(R) = \frac{\Delta\tau^o_{1R} - \Delta\tau^0_{2R}}{(\sigma_1 - \sigma_2)\Delta R}. \quad (9)$$

The relative uncertainty $\epsilon = \delta N_0/N_0$ depends on a large number of interrelated parameters and can be expressed as the sum of two terms, $\epsilon_1 + \epsilon_2$.

(1) ϵ_1 is the statistical error due to the signal and background noise fluctuations and is related to the signal uncertainty by

$$\epsilon_1 = \frac{1}{2\tau_R^o\sqrt{n_0}}(f_1^2 + f_2^2)^{1/2}, \tag{10}$$

where

$$K = \frac{\tau_R^o}{\Delta\tau_R^o} = \frac{\int_0^R N_0(R)dR}{N_0(R)\Delta R} \tag{11}$$

is the wavelength independent as far as one considers that the ozone absorption cross sections are altitude independent. One can also note that the product $K \cdot \Delta R$ does not depend on the range resolution of the lidar system;

$\tau_R{}^o =$ is the differential integrated optical thickness: $\tau_R{}^o = \tau_{1R} - \tau_{2R}{}^o$;

$n_0 =$ $A_0 \cdot \Delta R \cdot \xi \cdot \xi'/R^2$ is the wavelength-independent part of $N_{\lambda R}$;

$f\lambda$ is a wavelength-dependent function given by

$$f_\lambda^2 = \frac{\exp(2\tau_{\lambda 1})}{\beta_\lambda n_{e\lambda} P_\lambda \exp(-2\tau_{\lambda 1})}(\{1 + \exp[2(\tau_\lambda^o/K)]\} + X_\lambda^o(1 + 4\exp(\mu_{\lambda 1})\exp[4(\tau_{\lambda 1} + \tau_\lambda^o/K)]); \tag{12}$$

$$\mu_\lambda = \ln\left[\left(1 + \frac{\Delta R}{R}\right)\left(\frac{\beta_{\lambda 1}}{\beta_{\lambda 2}}\right)^{1/2}\right] + \Delta\tau_\lambda^e; \tag{13}$$

$$X_\lambda^o = \frac{n_B + n_D}{n_{\lambda 1}}\exp(-2\tau_\lambda^e); \tag{14}$$

P_λ is independent of the ozone absorption; and is the number of laser pulses emitted at wavelength λ.

(2) ϵ_2 is a systematic error due to the wavelength dependence of the scattering and absorbing (other than ozone) properties of the atmospheric medium which has been neglected in the derivation of Eq. (16). A general expression of ϵ_2 has been given by Megie and Menzies[3] as

$$\epsilon_2 = \frac{K \cdot \Delta R}{\tau_R^o} \cdot G(R,\lambda) \cdot \frac{\Delta\lambda}{\lambda_1}, \tag{15}$$

where $G(R,\lambda)$ is a function of range and wavelength depending on the scattering and extinction properties of the atmospheric gas and particles, written as

$$G(R,\lambda) = 2\left(1 - \frac{m}{4}\right)\frac{1 - r_{\lambda R}}{(r_{\lambda R})^2}\left(\frac{1}{h} - \frac{1}{H}\right) + m\alpha_\rho + {}^4\alpha_M. \tag{16}$$

Using these expressions of the various uncertainties an error analysis of the DIAL measurement taking into account both experimental parameters and atmospheric characteristics can now be performed. A minimum value of ϵ can be obtained for a given range by an appropriate choice of the laser emission wavelength λ_1 and λ_2. In the general case, this optimization of the DIAL measurement requires a numerical computation to include the experimental parameters of the lidar system and the atmospheric parameters related to molecular and aerosol scattering and ozone absorption. The description of such computations is beyond the scope of this paper and here we only consider the higher altitude ranges, above 2 km. A detailed analysis of ozone measurements in the boundary layer can be found in Pelon and Mégie.[4]

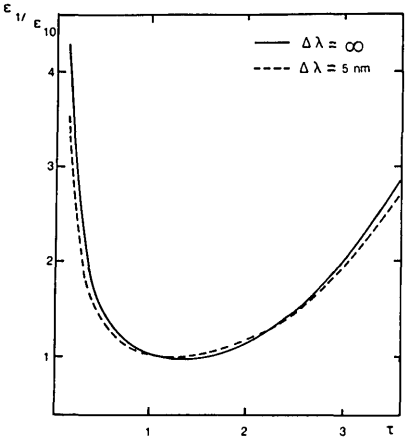

Fig. 1. Altitude dependence of the optimum wavelength λ (in nm), which minimizes the statistical error ϵ, for each altitude level ($\Delta\lambda = \infty$).

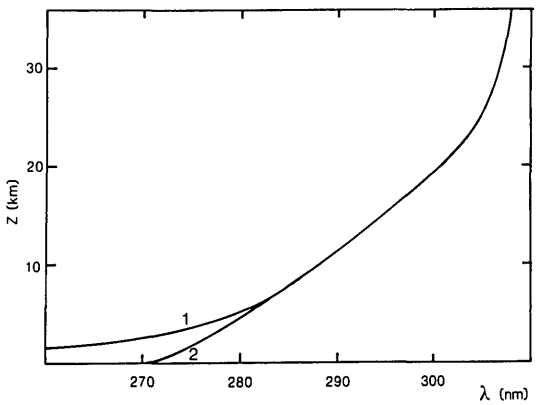

Fig. 2. Variations of the statistical error ϵ, relative to its minimum value ϵ_{10} (obtained for $\tau_{10}^0 = 1.1$) as a function of the on-line optical thickness τ_{10}: curve 1, $\Delta\lambda = \infty$; curve 2, $\Delta\lambda = 5$ nm.

A. Upper Troposphgeric and Stratospheric Measurements

Above 2 km, ϵ_2 decreases rapidly with altitude, for average values of higher tropospheric and stratospheric aerosol content. The choice of operating wavelengths is then determined by calculating the minimum value of ϵ_1 as a function of the three interrelated and wavelength-dependent parameters τ_{1R}^o, τ_{2R}^o, $\Delta\lambda$. For a given value of the larger absorption wavelength λ_1, the minimum is obtained for $\tau_2^o = 0$. This condition cannot be experimentally achieved in the case of the ozone UV absorption bands, which present continuous absorption features over a wide wavelength range. Thus the optimization procedure will consist of first calculating the value of $\tau_{1R}{}^o$ and thus λ_1, corresponding to the minimum value of ϵ_1 for $\Delta\lambda = \infty$ (Fig. 1), and then

evaluating the decrease in accuracy that results from the choice of a finite value of $\Delta\lambda$ compatible with both the experimental constraints and a maximum value of ϵ_2. Mégie and Menzies[3] have shown that the optimum value of τ_{1R}^0 is 1.28, in the case of a shot-noise limited signal when one neglects the off-line (λ_2) absorption (for ozone measurements this corresponds to large values of $\Delta\lambda$). In Fig. 2 we have represented the variations of ϵ_1 relative to its minimum value ϵ_{10} obtained for $\tau_{10} = 1.1$ as a function of τ_{10}. The values of the atmospheric density as a function of altitude required for the calculations were taken from the U.S. Standard Atmosphere.[8] By comparing these variations with the ones obtained for ϵ_2, one can show that the optimum wavelength interval has to be in the 5–15-nm range. The final choice of 5 nm has been adopted by considering the maximum tuning range of the laser systems and the possibility of using several wavelength pairs for the measurement within this range.

The optimum value of λ_1 as determined above is only valid for a given altitude range R. From an experimental point of view, it seems impossible to use as many wavelength pairs as the number of altitude levels of the measurement. Therefore, we have calculated the altitude variations of $\epsilon_1(\lambda_1,\Delta\lambda)$ by using the mean ozone profile of Krueger and Minzer[9] typical of mid-latitude regions. These relative variations represented on an arbitrary scale, corresponding to experimental conditions, are given in Fig. 3 for three wavelength pairs (λ_1,λ_2). The shorter wavelengths are used to probe the lower altitude levels, and the useful range of a given pair can be extended up to 7–8 km so that the measurement accuracy stays between its optimum value ϵ and 1.2 ϵ.

B. Upper Stratospheric Measurements and Ozone Total Content

Attempts to measure ozone number density above its maximum using a ground-based UV system are complicated by the high extinction rate of the laser emitted light due to absorption in the lower altitude levels. Furthermore, the rapid decrease in the ozone number density above 28 km requires rapidly increasing acquisition times for the measurement. The choice of higher wavelengths (wavelength pair B with $\lambda_1 = 305.8$ nm and $\lambda_2 = 310.8$ nm when using a Nd:YAG pumped dye laser or with $\lambda_1 = 308$ nm and $\lambda_2 = 355$ nm when using an Exciplex laser; see Sec. III) allows us to overcome these major problems and to probe the upper levels with appropriate integration times for geophysical applications.[10] The ozone total content can also be derived from the measured vertical distribution using a combination of the two wavelength pairs (pair A at lower altitudes, 288–294 nm; pair B at higher levels). Various sources of uncertainty have to be considered:

Statistical fluctuations of the detected signals which constitute the major error source, estimated to be <10 Dobson units in a 95% confidence interval. This error can be further reduced by increasing the acquisition time.

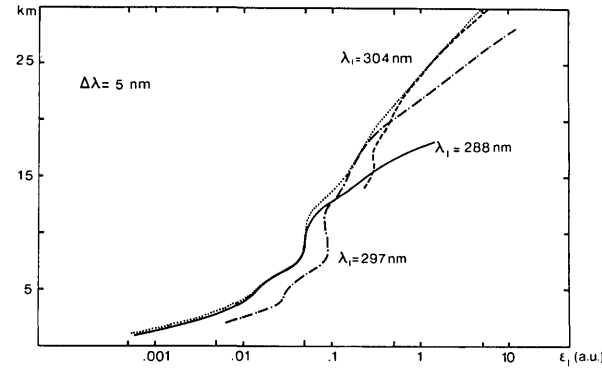

Fig. 3. Variation of the statistical error ϵ_1 as a function of $\Delta\lambda$ for different optical thicknesses τ_{1R}^0 corresponding to different wavelengths λ or ranges. ϵ_1 is normalized to its minimum value (from Ref. 4).

Rayleigh extinction by the atmospheric gas molecules: this uncertainty is reduced below 0.1 Dobson unit by correcting the lidar data using the pressure, temperature, and humidity distribution measured by radiosonde or lidar measurements.

Mie differential extinction by aerosol particles: this uncertainty, which can be large at lower altitudes, is reduced when using the A wavelength pair to measure the total content up to 15 km which leads to high ozone optical thickness compared to the aerosol contribution. It can be estimated to be <1 Dobson unit whereas the use of the B pair in the same altitude range will have resulted in a 1 order of magnitude higher uncertainty.

A constant value of 10.4 Dobson units which corresponds to the average ozone content above 40 km[9]; the 2σ standard deviation results in a 3.2 Dobson unit uncertainty.

C. Interference with Other Absorbing Gases

Two minor constituents have to be considered as potential interference absorbers in the 300-nm wavelength range:

Sulfur dioxide: SO_2 absorption spectrum presents a band structure with a spectral width for the individual features of 1 nm.[11] The differential cross section between an absorption maximum and a minimum ($\Delta\lambda \sim 1.5$ nm) can reach 10^{-18} cm^2. In the case of large amounts of SO_2 in the troposphere over urban areas, the corresponding differential absorption coefficient can reach values as large as 0.1 km^{-1} at the ground level.[12] To avoid any interference, the two laser wavelengths λ_1 and λ_2 should be chosen so that the SO_2 differential absorption vanishes. This choice is always possible within 0.3 nm of a predetermined wavelength.

Nitrogen dioxide: NO_2 presents in the same wavelength range absorption bands with cross-sectional values[13] of the order of 10^{-19} cm^2. The differential cross section for a 5-nm wavelength interval is then 2.5×10^{-20} cm^2. It results, if one considers the higher mixing ratios typical or urban of polluted areas (~0.3

ppm),[14] in a differential absorption coefficient of 0.015 km^{-1} at the ground level. The corresponding error on the ozone measurement will be 2% and can be taken care of by the same procedure as for SO_2.

In any case, the high altitude measurements will not be affected due to the very low atmospheric content in these interfering species above the boundary layer.

D. Temporal Variations of the Scattering Medium

If the two wavelengths are not simultaneously emitted, variations in the optical properties of the scattering medium might occur between the two laser shots, owing to atmospheric transport. This will be of particular importance at lower altitudes if the aerosol content is high or at the tropopause level in the presence of cirrus clouds. Thus, even if the integration time required for the measurement is large, the switching between the two wavelengths will have to be made with a time constant much smaller than the time constant characteristic of the dynamical transport. The experimental system will have to take this requirement into account (see Sec. III), and the possible design of a dual cavity laser emitting simultaneously at two wavelengths should also be investigated.

E. Altitude Dependence of the Ozone Absorption Cross Sections

The values of the absorption cross sections that we used to derive the ozone number densities are taken from Inn and Tanaka.[15] The spectral resolution of their measurements is lower than the resolution of the lidar measurements as given by the laser linewidth (~50,000). The assumption has thus to be made that the mean value of the absorption cross section is the same over these different wavelength intervals. This is not experimentally confirmed, but the precise knowledge of the emitted wavelength (see the following subsection) will also allow us to correct data from this systematic error using high resolution absorption spectra of ozone which have become available in this wavelength range very recently.[16]

The ozone absorption cross sections are temperature dependent mainly in the Huggins bands above 310 nm where variations as large as a factor of 2 can be observed for a 100 K temperature difference. Low resolution measurements[17] have shown that the absorption minima are more sensitive than the maxima to the temperature variations. In the Hartley bands, the relative temperature variation of the cross section is much lower: 1% for a 10 K variation.[16,17] Therefore, the use of an atmospheric model to take into account this temperature dependence of the absorption cross section and an *a posteriori* control using the radiosonde measurements of the nearby meterological stations will reduce this uncertainty on the ozone profile to <0.5%.

III. Experimental Systems

The system evaluation conducted in the previous section shows that the measurement of the ozone number density profile by the DIAL technique is achievable using presently available laser systems with a temporal resolution compatible with scientific geophysical objectives. Two altitude domains might be considered.

Below 30 km and due to the presence of aerosol layers in the troposphere and stratosphere a dual wavelength operation is requested with a wavelength interval between the two emitted laser lines not larger than 5 nm.

Above 30 km where the atmosphere can be generally considered as purely molecular—whereas after large volcanic eruptions aerosol layers have been observed up to 40 km—a single wavelength lidar might give information on the ozone profile. However, such a determination implies the use of an atmospheric density model which can lead to uncertainties in the ozone values especially during perturbed conditions. This difficulty might be overcome, again using a second laser emitted wavelength but with the possibility of an increased wavelength interval.

A. Transmitter

The design of an experimental system must also take into account the available laser sources. Two types of laser are presently potential candidates for such a system:

Frequency-doubled dye lasers pumped by a Nd^{3+}:YAG laser which have the advantage of being tunable over a broad wavelength range but are somewhat limited in terms of available output power.

Exciplex lasers which are frequency fixed on a given transition of the active medium but can emit large average and peak powers.

Both lasers have been used for the measurements of atmospheric ozone. The first and as yet only ground-based lidar system using dye lasers has been operational at the Observatoire de Haute Provence since 1977.[4,10,18] The active part of the transmitter is a laser-pumped frequency-doubled dye laser. The pump laser is a Nd^{3+}:YAG laser (Quantel model 480) emitting an energy of 750 mJ at 1.06 μm with a repetition rate of 10 Hz. This IR emission is frequency doubled with an efficiency of 40% resulting in an available pump energy of 300 mJ at 0.53 μm. The transversely pumped dye laser (Jobin Yvon model HPHR) includes one oscillator cavity and three amplifier stages.[19] To cover the wavelength range from 570 to 620 nm, two dye solutions are used as the active medium (1) between 570 and 600 nm, a 5×10^{-4} M/liter solution of Rh6G in water plus 5% ammonix; (2) between 590 and 620 nm, a 5×10^{-4} M/liter solution of Rh610 in water plus 5% ammonix.

The energy conversion efficiency is 40% corresponding to an output energy of 120 mJ. The wavelength selection and spectral narrowing of the emitted laser line are made by using a 2750-groove mm^{-1} grating at Littrow incidence. The emission characteristics of this laser are summarized in Table I. To adapt these characteristics to the requirements brought out from Sec. II, two experimental achievements remain to be made:

Table I. Characteristics of Lidar Systems in Operation at the Observatoire de Haute Provence for Lidar Measurements of the Ozone Vertical Distribution

	Nd^{3+}:YAG pumped	Exciplex laser/ Nd^{3+}:YAG laser
Emitter		
Output energy	20 mJ	250 mJ (λ_{on})–200 mJ (λ_{off})
Repetition rate	10 Hz	20 Hz
Pulse duration	15 nsec	15 nsec
Emitted wavelength	280–310 nm	308 nm (λ_{on})–355 nm (λ_{off})
Emission linewidth	5 pm	0.7 nm
Beam divergence	5×10^{-4} rad	10^{-3} rad
Receiver		
Telescope diameter	80 cm	
Telescope field of view	2×10^{-3} rad	
Receiver bandwidth	70–3 nm	

The output wavelength must be converted to a value in the near-UV wavelength range by second harmonic generation using a KDP crystal. Owing to the high peak power of the fundamental emission (20 MW) the energy conversion efficiency is close to 35%. The output energy between 285 and 310 nm is within the 10–20-mJ range.

The laser system has to emit sequentially two wavelengths. It is designed so that the full sequence of wavelength switching is automatic. The output wavelength of the dye laser fundamental emission is monitored by using a spectrometer and a Fizeau interferometer, giving patterns recorded on diode arrays. A computer-controlled servomechanism[20] is used to both ensure the stability of the output wavelength from λ_1 to a second preprogrammed value λ_2. To allow this switching to be fast ($t \leq 1$ sec) and to avoid the experimental difficulties connected with the accuracy of the doubling crystals positioning as a function of wavelength, two KDP crystals are used that are preset to the optimum value of the phase matching angle for λ_1 and λ_2. The laser beam is then mechanically switched from one crystal to the other, depending on the incident wavelength. When a second wavelength pair has to be used, the values of λ_1 and λ_2 as programmed for the servo control loop are changed so that the crystal angles. By using this system, the stability of the laser emission wavelength is better than 1 pm and the switching operation takes place in <0.5 sec. As the laser divergence is smaller than 5×10^{-4} rad, no transmitting optics is used and the beam is sent directly upward by using a total reflection prism.

Exciplex lasers for ozone measurements were first put into operation by Uchino *et al.*[21] who used an XeCl laser emitting at 308 nm. The maximum output energy was 120 mJ/pulse for the first system developed with a rather low repetition rate of 0.1 pulse/sec so that the average power is of the same order of magnitude as for the dye laser. However improvement of these systems has now led to XeCl laser sources with output energy in the 200-mJ range and repetition rates up to 50 Hz.[22,23] Dual wavelength systems are presently in operation which use either SRS generation or a third harmonic:

Stimulated Raman scattering generation. The 308-nm radiation is focused into a high-pressure methane cell to generate the reference line (off absorption). The wavelength interval is then equal to 2880 cm^{-1} leading to an emission at 338 nm which is absorbed less significantly by ozone. The conversion efficiency is 15% for a pressure of 35 atm and a focusing length of 125 cm. The two lines can be emitted simultaneously.[22]

The third harmonic of a Nd^{3+}:YAG laser at 355 nm then requires an additional laser source.

In both cases the large wavelength interval (30–40 nm) allows only measurement above 25 km if aerosol-free conditions can be assumed. The last configuration was used at the Observatoire de Haute Provence in September 1983 to measure the upper stratospheric ozone vertical distribution during the MAP/Globus campaign.[23] The characteristics of the laser emitter are summarized in Table I.

B. Optical Receiver Electronic Processing and Data Acquisition

These parts of the lidar system are similar for the various laser systems which have been used up to now (see Table I). The following description refers to the system presently in use at the Observatoire de Haute Provence. The backscattered signal is collected by an 80-cm diam telescope in a Cassegrain configuration. The distance between the emitting point and the telescope axis can be varied, depending on the altitude range of the observations to increase or decrease the range at which the fields of view of the transmitter and the receiver begin to overlap. This will avoid saturation of the photomultiplier tube from the low altitude backscattered signals. The telescope field of view is adjusted by using a remotely controlled iris and can thus be reduced to its limit value compatible with the laser divergence. The spectral bandwidth of the receiver can be reduced by either using a wideband interference filter (70 nm) or several narrow bandwidth interference filters (3 nm) which can be automatically changed when the laser emission wavelengths are changed. The signal is detected by using a photomultiplier tube. The dynamic range of the backscattered signal between the ground and 30 km can be as large as 10^6 according to Eq. (2); two acquisition modes are thus used:

For the lower altitude range the electrical signal delivered by the PMT is analyzed by using a transient waveform recorder (Biomation 1010) with a sampling frequency of 10 MHz, which corrresponds to a maximum altitude resolution of 15 m. A 10-bit converter is used for the analog-to-digital conversion.

For the altitude levels above 10–12 km, a 256-channel photon counter is used in parallel with the transient recorder, so that the two acquisition modes overlap with respect to the altitude range. The time gate of the photon counter can be varied from 1 to 8 μsec and the maximum altitude resolution is thus 150 m.

The data provided by the two acquisition systems are then fed into a PDP 11-34 computer and are stored

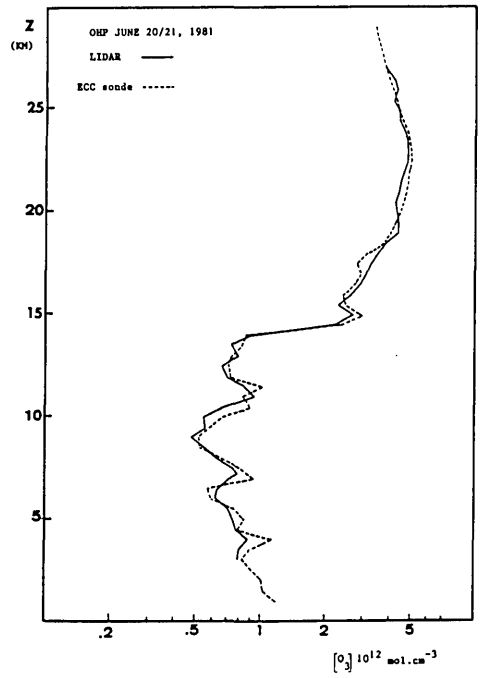

Fig. 4. Vertical ozone distribution as measured by an ECC sonde and lidar at the Observatoire de Haute Provence (June 1981) (from Ref. 4).

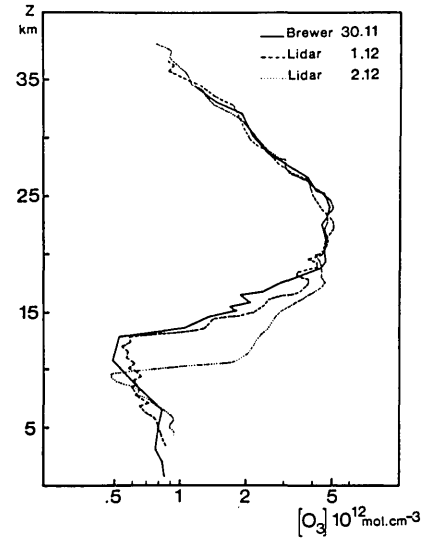

Fig. 5. Ozone concentration profile measured by lidar at the Observatoire de Haute Provence (44°N, 50°E) on 1 Dec. 1981 (dashed line) and 2 Dec. 1981 (dotted line) at 0-h UT compared with the profile obtained by a Brewer Mast sonde launched at Bisacrosse (44°N, 0,5°W) on 30 Nov. 1981 (solid line) (from Ref. 10).

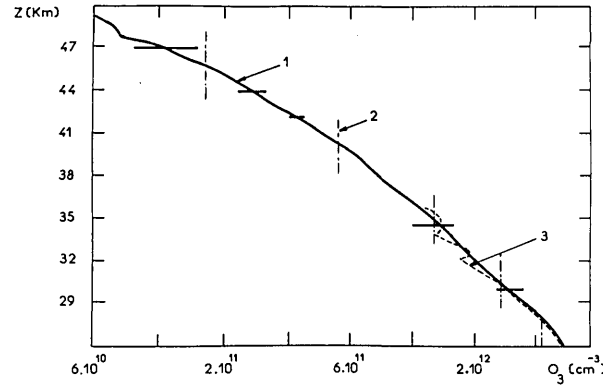

Fig. 6. Vertical distribution of ozone concentration in the upper stratosphere (25–50 km) as measured by XeCl lidar (solid line), Brewer Mast sondes (dotted line), and the Umkehr technique (solid vertical lines) at the Observatoire de Haute Provence. The statistical errors are shown for each system.

on a floppy disk. A presummation of the single laser shot signals is made to reduce the volume of stored data. The PDP 11-34 computer is used to control the full sequence of a DIAL measurement. The experimental parameters (acquisition time, altitude resolution, values of the various laser wavelengths, switching time, etc.) are typed in to automatically start the sequence of laser firings. During the experiment, the laser energy and emission wavelengths are continuously monitored, and the data acquisition takes place only if all these parameters are within the range of predetermined values.

IV. Results of DIAL Ozone Measurements

The reliability of the various systems presented here for ozone monitoring has been tested on an operational basis for the last three to four years. As a result the DIAL technique has proved its ability to provide altitude profiles of ozone number density from the ground up to 50 km at the present.

The measurements performed at the Observatoire de Haute Provence using dye lasers as the transmitter are obtained in successive steps within integration time of the order of 1 h. The profiles shown in Figs. 4 and 5 correspond to the 0–17-km and 15–40-km altitude ranges and are obtained sequentially. This experimental procedure results from the wavelength optimization as a function of height. The first profile is obtained within 15 min with a relative accuracy of better than 5% for a vertical resolution of 450 m. The higher altitude profile requires an integration time of ~45 min. The vertical resolution decreases from 1 km at 25 km to 3 km at 35 km and above. Here again the 1σ standard deviation is better than 5% up to 25 km and decreases down to 20% at the uppermost level. Several comparisons with *in situ* measurements have been made.[24] The results show good agreement between *in situ* and remote sensing instruments.[25,26]

Similar compositions with balloon-borne ozonesondes have also been performed by Uchino *et al.*[27] covering the altitude range of XeCl measurements between 15 and 30 km. Here again the agreement is rather good. The XeCl laser developed by Rothe *et al.*[22] has been implemented at a high altitude (3-km asl) station at the top of the Zigspitze in the German Alps. This system has been in operation since the winter of 1982 and provides high altitude measure-

Table II. Errors Related to Lidar Measurements of the Ozone Vertical Distribution for Various Altitude Ranges and Emitters (see Table I)

Systematic errors		Ozone vertical distribution	Ozone total content
Uncertainty on the ozone absorption cross sections absolute values		±3%	±3%
Temperature dependence on the ozone cross sections with correction using lidar/radiosonde data		≤0.3%	≤0.3%
Influence of the laser linewidth fluctuations		≤0.1%	≤0.1%
Rayleigh extinction and scattering corrected from lidar/radiosonde data	0–25 km (290–295 nm)	≤0.4%	≤0.3%
	25–50 km (305–310 nm)	≤0.15%	
Mie extinction and scattering corrected using lidar data and aerosol models	0–30 km	≤1%	≤0.4%
	30–50 km	≤0.3%	
Absorption by minor constituents in nonpolluted areas		≤0.1%	≤0.1%
Residual ozone			Z_{max} = 36 km ≤ 0.8% Z_{max} = 50 km ≤ 0.2%

Statistical errors (integrated time required for a 3% accuracy)

	5 km	10 km	15 km	20 km	25 km
Nd^{3+}:YAG pumped dye laser (E ~ 40 mJ–ΔZ = 1 km)	≤1 min	2 min	15 min	80 min	5 h
	25 km	30 km	35 km	40 km	45 km
Exciplex laser (E ~ 250 mJ–ΔZ = 3 km)	≤1 min	1 min	15 min	1 h	4 h

ments between 30 and 50 km which have also been compared with classical measuring techniques.[28] As already mentioned, a similar system was also operated at the Observatoire de Haute Provence in September 1983 and comparison of the ozone vertical profile obtained by lidar Brewer Mast sonde and Umkehr measurements are shown in Fig. 6 in the 25–50-km altitude range.[23]

One of the first applications of ground-based lidar systems for ozone measurements is the monitoring of the ozone vertical distribution on a routine basis. The altitude extension of the lidar measurements up to the 50-km level will allow the study of long-term ozone variations in a region where the potential effects of man-made activities are maximum due to catalytic cycles involving chlorine species in particular. With respect to passive systems now in use the lidar system has several advantages:

control of the emitting source which results in a possible independent autocalibration of each system,

possibility by careful choice of emitting wavelengths to avoid interferences by aerosols, sulfur dioxide, or nitrogen dioxide, and

direct altitude resolution of the system.

Table II summarizes the expected accuracies for ozone distribution and ozone total content measurements and emphasizes the requested corrections which can be provided by simultaneously obtained additional lidar determinations of the temperature and aerosol contents.

Several studies have also been undertaken using lidar data which refer to various temporal and spatial scales. For example, short-term variability of the ozone number density below 16 km has been observed by Pelon and Megie[4]: successive profiles recorded during the night show a twofold increase in the ozone number density at 10 km within a 4-h period of time. Such ozone variations, already observed by other techniques[29] are related to horizontal transport at the tropopause level. For such studies the temporal continuity in the observations which characterizes the lidar systems is of great advantage as it allows a determination of the horizontal extension of such ozone structures with a very high spatial accuracy. The increase in the temporal resolution of the lidar measurements at the tropopause level allows integration times of the order of a few minutes which lead to the determination of time–height isocontours of the ozone number density as a function of time as shown in Fig. 7. These measurements were obtained at the Observatoire de Haute Provence during the night of 3 Dec. 1981 and give evidence for an ozone concentration increase between 6 and 8 km. The temporal and spatial scales associated with this event are related, as shown from a synoptic analysis of the meteorological charts, with a moving cold front and the associated intrusion of stratospheric air into the troposphere at the junction between the front and the tropopause boundary.[23]

Large variations in ozone number density are also observed on a day-to-day basis. They are related to larger scale horizontal transport. Such increases of the ozone concentration at the tropopause level have been observed on several occasions during field experiments. The altitude of the ozone bulge may vary from

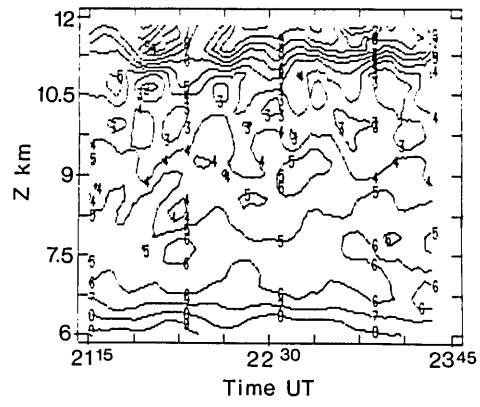

Fig. 7. Isocontours of the ozone number density (in 10^{11} cm^{-3}) as a function of altitude (vertical axis) and time in minutes for a 3-h period of time starting at 22:00 on 3 Dec. 1981 at the Observatoire de Haute Provence.

10 to 12 km down to 6–8 km; in the latter case the peak concentration decreases when the bulge is observed at lower altitudes. From the meteorological network data, one can show that these increases are systematically correlated with a 2–3-km decrease of the tropopause height corresponding to the presence of warmer air at these levels over southern France. A detailed analysis of one of these situations (July 1980) has already been performed by using the meteorological charts at various altitude levels in the troposphere and lower stratosphere.[30] For such events the potentiality of a ground-based system can be fully utilized as shown by the study of Uchino *et al.*[27] which gives evidence for a high positive correlation between the ozone column density in the 15–25-km altitude range with the total ozone observed by a nearby Dobson spectrophotometer. Other correlations have also been studied by the same group such as a high positive correlation with temperature at 17–25 km, all these features being closely related to dynamical movements at the tropopause height.[26]

V. Conclusion

Due to the rapid development of powerful laser sources in the UV wavelength range which includes Nd:YAG pumped dye lasers and Exciplex lasers, ground-based lidar systems are now operational for ozone monitoring in the troposphere and the stratosphere. They can provide a direct measurement of the ozone vertical distribution from the ground up to the 50-km altitude level. Such systems will certainly play an important role in the determination of long-term ozone trends in the photochemical region and thus in the evaluation of anthropogenic effects in the earth's environment. Furthermore, the unique capacities of an active lidar system in terms of high temporal and spatial resolution and measurement continuity allow the observation of the ozone variations at various time and space scales which are of importance in such present-day areas of interest as troposphere–stratosphere exchanges, long-range transport and global budget of ozone or correlations between ozone number densities, and other atmospheric parameters. Considering the already operational character of the lidar systems, in the very near future they will constitute the basis for development of a new ground-based network for middle atmospheric observations of ozone.

This work was supported by grants from the Ministère de l'Environnement, CNRS (ATP Atmosphère Moyenne) and INAG. The authors are indebted to their colleagues of the Department of Atmospheric Physics and Dynamics at the Service d'Aéronomie for their help with the data acquisition and processing and for fruitful discussions.

This paper is based on one presented at the OSA Topical Meeting on Optical Remote Sensing of the Atmosphere, Incline Village, Nev., 15–18 Jan. 1985.

References

1. R. M. Schotland, "The Determination of the Vertical Profile of Atmospheric Gases by Means of a Ground-Based Optical Radar," in *Proceedings, Third Symposium on Remote Sensing of the Environment* (Environmental Research Institute of Michigan, Ann Arbor, 1964).
2. R. L. Byer, and M. Garbuny, "Pollutant Detection by Absorption Using Mie Scattering and Topographic Targets as Retroreflectors," Appl. Opt. **12,** 1496 (1973).
3. G. Megie and R. T. Menzies, "Complementarity of UV and IR Differential Absorption Lidar for Global Measurements of Atmospheric Species," Appl. Opt. **19,** 1173 (1980).
4. J. Pelon and G. Megie, "Ozone Monitoring in the Troposphere and Lower Stratosphere: Evaluation and Operation of a Ground Based Lidar Station," J. Geophys. Res. **87,** C7, 4947 (1982).
5. O. Uchino, M. Maeda, and M. Hirono, "Applications of Excimer Lasers to Laser-Radar Observations of the Upper Atmosphere," IEEE J. Quantum Electron. **QE-15,** 1094 (1979).
6. M. P. McCormick and T. J. Swissler, "Stratospheric Aerosol Mass and Latitudinal Distribution of the El Chichon Eruption Cloud for October 1982," Geophys. Res. Lett. **10,** 877 (1983).
7. R. M. Schotland, "Errors in the Lidar Measurement of Atmospheric Gases by Differential Absorption," J. Appl. Meteorol. **13,** 71 (1974).
8. *U.S. Standard Atmosphere* (U.S. GPO, Washington, D.C., 1976), 227 pp.
9. A. J. Krueger and R. A. Minzer, "A Mid-Latitude Ozone Model for the 1976 U.S. Standard Atmosphere," J. Geophys. Res. **81,** 4477 (1976).
10. J. Pelon and G. Megie, "Ozone Vertical Distribution and Total Content as Monitored Using a Ground Based Active Remote Sensing System," Nature London **299,** 137 (1982).
11. R. T. Thompson, J. M. Hoell, and W. R. Wade, "Measurements of SO_2 Absorption Coefficients Using a Tunable Dye Laser," J. Appl. Phys. **46,** 3040 (1975).
12. R. D. Stewart, S. Hameed, and J. Pinto, "The Natural and Perturbed Troposphere," IEEE Trans. Geosci. Electron. **GE-16,** 30 (1978).
13. A. M. Bass, A. E. Ledford, and A. H. Laufer, "Extinction Coefficients of NO_2 and N_2O_4," J. Res. Natl. Bur. Stand. Sect. A **80,** 143 (1976).
14. J. H. Seinfeld, *Air Pollution–Physical and Chemical Fundamentals* (McGraw-Hill, New York, 1975).
15. E. C. Y. Inn and Y. Tanaka, "Absorption Coefficient of Ozone in the Ultraviolet and Visible Regions," J. Opt. Soc. Am. **43,** 870 (1953).

16. A. M. Bass, "Ultraviolet Absorption Cross Sections of Ozone: Measurement Results and Error Analysis," in *Proceedings, Quadrennial Ozone Symposium*, Halkidiki, Greece (Reidel, Hingham, Mass., 1984), p. 7.2.
zone," Ann. Phys. Paris **72,** 709 (1953).
18. G. Megie, J. Y. Allain, M. L. Chanin, and J. E. Blamont, "Vertical Profile of Stratospheric Ozone by Lidar Sounding from the Ground," Nature London **270,** 329 (1977).
19. F. Bos, "Versatile High-Power Single-Longitudinal-Mode Pulsed Dye Laser," Appl. Opt. **20,** 1886 (1981).
20. C. Cahen, J. P. Jegou, J. Pelon, P. Gildwarg, and J. Porteneuve, "Wavelength Stabilization and Control of the Emission of Pulsed Dye Lasers by Means of a Multibeam Fizeau Interferometer," Rev. Phys. Appl. **16,** 353 (1981).
21. O. Uchino, M. Maeda, T. Shibata, M. Hirono, and M. Fujiwara, "Measurement of Stratospheric Vertical Ozone Distribution with a Xe–Cl Lidar: Estimated Influence of Aerosols," Appl. Opt. **19,** 4175 (1980).
22. K. W. Rothe, H. Walther, and J. Werner, "Differential Absorption Measurements with Fixed Frequency IR and UV Lasers," in *Optical and Laser Remote Sensing*, D. K. Killinger and A. Mooradian, Eds. (Springer-Verlag, New York, 1983).
23. J. Pelon and G. Megie, "Lidar Monitoring of the Ozone Vertical Distribution in the Troposphere and Stratosphere," in *Proceedings, Twelfth International Laser Radar Conference*, G. Mégie, Ed. (Aix en Provence, France, 1984), pp. 247–250.
24. M.L. Chanin, "The Intercomparison Campaign Held in France in June 1981: Description of the Campaign," Planet. Space Sci. **31,** 707 (1983).
25. G. Megie and J. Pelon, "Measurements of the Ozone Vertical Distribution (0–25 km): Comparison of Various Instruments, GAP-Observatoire de Haute Provence, June 1981," Planet. Space Sci. **39,** 791 (1983).
26. J. Pelon and G. Megie, "Lidar Measurements of the Vertical Ozone Distribution During the June 1981 Intercomparison Campaign GAP/OHP," Planet. Space Sci. **31,** 717 (1983).
27. O. Uchino, M. Maeda, H. Yamamura, and M. Hirono, "Observation of Stratospheric Vertical Ozone Distribution by a XeCl Lidar," Appl. Phys. Lett. **33,** 807 (1978).
28. J. Werner, K. W. Rothe, and H. Walther, "Measurements of the Ozone Profile up to 50-km Altitude by Differential Absorption Laser Radar," in *Proceedings, Quadrennial Ozone Symposium*, Halkidiki, Greece, 3–7 Sept. 1984 (D. Reidel, Hingham, Mass., 1985), 842 pp.
29. H. U. Dutsch, "Vertical Ozone Distribution and Tropospheric Ozone," in *Proceedings, NATO Advanced Study Institute on Atmospheric Ozone*, M. Nicolet and A. C. Aikin, Eds. (U.S. Department of Transportation, Washington, D.C., 1979).
30. J. Pelon, P. Flamant, M. L. Chanin, and G. Megie, "Intrusion d'ozone d'origine polaire aux latitudes moyennes: Mise en évidence par sondage laser," C.R. Acad. Sci., **292,** 319 (1981).

Meetings Calendar

1985

November

3–8	APS Div. of Plasma Physics Mtg., San Diego *Amer. Physical Soc., 335 E. 45th St., N.Y., N.Y. 10017*
4–8	Laser Fundamentals & Systems course, Orlando *Eng. Tech., Inc., P.O. Box 8859, Waco, TX 76714*
6–7	Regional Color & Appearance course, Atlanta *Hunterlab., 11495 Sunset Hills Rd., Reston, VA 22090*
11–14	4th Int. Congr. on Applications of Lasers & Electro-Optics, San Francisco *Laser Inst. of Am., 5151 Monroe St., Suite 118W, Toledo, Ohio 43623*
11–15	Remote Sensing for Geologists & Geophysicists course, San Francisco *A. Goetz, P.O. Box 7, Altadena, Calif. 91001*
11–15	Photographic Science course, Rochester *W. Siegfried, RIT, P.O. Box 9887, Rochester, N.Y. 14623*
13–15	3rd Int. Conf. on Future of Optical Memories, Compact Discs, & Videodisks, San Francisco *TOC, P.O. Box 14817, San Francisco, CA 94114*
17–22	25th SPSE Fall Symp., Arlington *SPSE, 7003 Kilworth La., Springfield, Va., 22151*
18–22	Synthetic Aperture Radar With Remote Sensing Applications course, Wash., D.C. *Cont. Eng. Ed. Program, Geo. Wash. U., Wash., D.C. 20052*
18–22	Laser Safety course, Orlando *Eng. Tech., Inc., P.O. Box 8859, Waco, TX 76714*
19–22	Eastern Analytical Symp., New York *D. Klein, EAS Publicity, Merck & Co., Inc., P.O. Box 2000/R80L-106, Rahway, N.J. 07065*
20–21	Regional Color & Appearance course, Newark *Hunterlab., 11495 Sunset Hills Rd., Reston, VA 22090*
25–6 Dec.	2nd Int. Conf. on Optical & Electro-Optical Applied Science Eng., Cannes *SPIE, P.O. Box 10, Bellingham, Wash. 98227*

December

1–4	Electron Devices Int. Mtg., Wash., D.C. *M. Widerkehr, Courtesy Assoc., Inc., 655 15th St., N.W., Ste. 300, Wash., D.C. 20005*
2–4	**Optical Bistability OSA Top. Mtg.,** Tucson *OSA Mtgs. Dept., 1816 Jefferson Pl., N.W., Wash., D.C. 20036*
2–5	Opto-Electronic Imaging Int. Symp., Dehra Dun *O. Nijhawan, Instruments Res. & Development Establishment, Dehra Dun-248 008, India*

continued on page 3496